Correction of ultraviolet single photon counting image distortion

Xinghua Zhang (张兴华)[1,2], Baosheng Zhao (赵宝升)[1], Zhenhua Miao (缪震华)[1,2], Wei Li (李 伟)[1,2], Xiangping Zhu (朱香平)[1], Yong'an Liu (刘永安)[1,2], and Wei Zou (邹 玮)[1]

[1]*State Key Laboratory of Transient Optics and Photonics, Xi'an Institute of Optics and Precision Mechanics, Chinese Academy of Sciences, Xi'an 710119*

[2]*Graduate University of Chinese Academy of Sciences, Beijing 100049*

Received March 14, 2008

Single photon counting imaging technology has been widely used in space environment detection, astronomy observation, nuclear physics, and ultraweak bioluminescence. However, the distortion of the single photon counting image will badly affect the measurement results. Therefore, the correction of distortion for single photon counting image is very significant. Ultraviolet single photon imaging system with wedge and strip anode is introduced and the influence factor leading to image distortion is analyzed. To correct original distorted image, three different image correction methods, namely, the physical correction, the global correction, and the local correction, are applied. In addition, two parameters, i.e., the position index and the linearity index, are defined to evaluate the performance of the three methods. The results suggest that the correction methods can improve the quality of the initial image without losing gray information of each counting light spot. And the local correction can provide the best visual inspections and performance evaluation among the three methods.

OCIS codes: 030.5260, 110.0110, 100.0100.

doi: 10.3788/COL20080609.0661.

With the development of space environment detection, biology medicine, and nuclear detection technology, single photon counting imaging technology[1−3] was applied widely in astronomical observation, biology fluorescent, and spectroscopic measurement[4−6]. The technology can provide not only the time information of a photon, but also the position information. However, the distortion of the original image badly affects the measurements. To resolve this problem, some measures are implemented to enhance the performance of the single photon imaging system. However, only by system improvement the distortion still exists at image edge. Therefore it is necessary to adjust the counting image by means of image processing.

In this letter, ultraviolet single photon imaging system with wedge and strip anode is introduced and the influencing factor leading to image distortion of the system is analyzed. In order to correct image distortion, three different image correction methods are applied. In addition, to evaluate the effect of the three methods, two parameters are defined to estimate the position distortion and linearity distortion of the corrected images.

Figure 1 is the sketch of the ultraviolet single photon imaging system. It consists of Hg lamp, filters, mask, microchannel plate (MCP), wedge and strip anode (WSA), charge sensitive amplifier (CSA), shaping amplifier, data acquisition card (DAQ), and computer. The mask, MCP, and WSA are in the vacuum chamber. The principle of the ultraviolet single photon imaging system can be described as follow. Firstly, the ultraviolet is weakened to single photon stream through some filters, the single photon stream irradiates the MCP surface and produces second electrons which are multiplied by MCP. Then, the electron cloud is collected via WSA. Next, the charge signal is converted to voltage signal through a CSA, which is shaped and filtered using shaping amplifier, and the

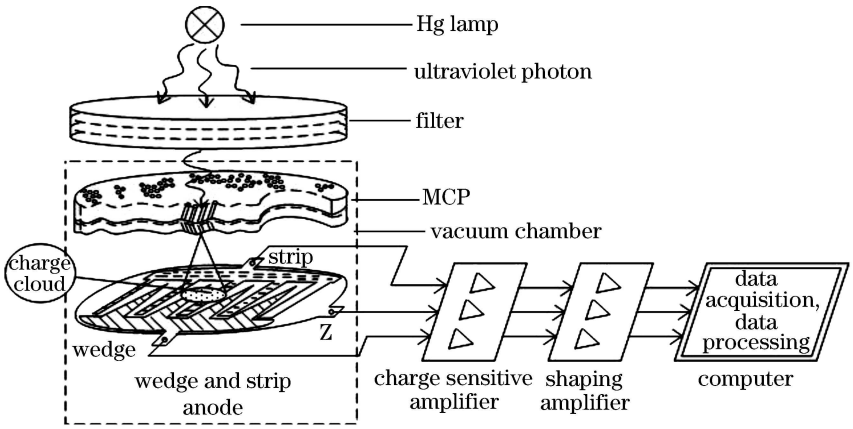

Fig. 1. Sketch of ultraviolet single photon imaging system.

1671-7694/2008/090661-04

output signal from shaping amplifier is acquired by DAQ. Finally, an ultraviolet single photon counting image is obtained through processing the acquired data.

In the whole image acquisition processes, there are mainly four reasons leading to the image distortion: the size of charge cloud[7], the actual shifts in the centroid of the charge cloud on its travel to the anode, the capacitive coupling between the discrete electrodes of the wedge and strip anode[8], and the nonlinearity in the amplification and conversion process of the electronics[9].

To obtain better original image, some steps are taken to optimize the ultraviolet single photon imaging system. Firstly, modulate the diameter of charge cloud by changing the distance between the output side of MCP and WSA. Secondly, add an appropriate electric field between output side of MCP and WSA to avoid the centroid shift of the charge cloud. Thirdly, optimize the design of WSA to reduce the capacitive coupling between the discrete electrodes of WSA[10]. Fourthly, decrease electronic noise and optimize electronic readout.

The ultraviolet single photon counting image is obtained based on the improvement above. Figure 2 shows the pinhole mask photo and the standard image getting from the mask. The pinhole mask is placed at the input side of MCP. After 30-min data accumulation and processing, an ultraviolet single photon counting image is obtained, as shown in Fig. 3. One can see that the original image is similar to the pinhole mask and the intensity of each light spot is not uniform. This is due to the counts are different at each pinhole. In addition, there are a few counts around the light spots because the ultraviolet light is not parallel incidence and the pinhole mask is not very flat after mechanical processing.

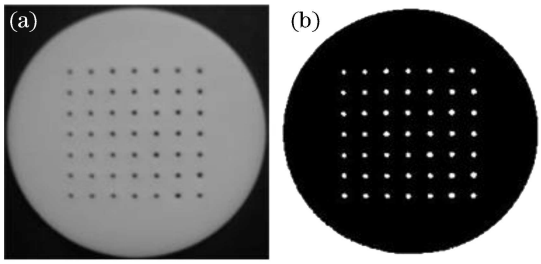

Fig. 2. (a) Photo of the forty-nine pinhole mask and (b) standard image obtained from (a).

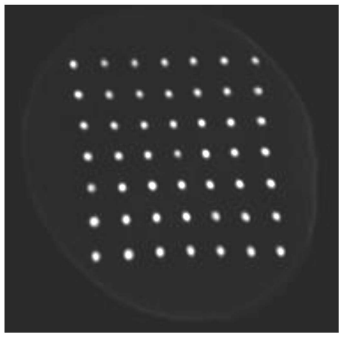

Fig. 3. Original single photon counting image.

Although some steps have been taken to improve the performance of the system, there is still distortion of the original image. To remove the image distortion, we adopt three different image processing methods to correct original image. The first correction method is the physical correction. Since capacitive coupling is a factor to affect image distortion, the image will be corrected by modulating capacitive coupling constants between electrode W-S, W-Z, and S-Z (W, S, and Z represent the electrodes of wedge, strip, and Z in Fig. 1, respectively). The relationship of the corrected coordinate (x', y') and the original coordinate (x, y) is[8,11]

$$x' = kX \cdot x + kfX \cdot (1 - x - y) + X_0, \tag{1a}$$

$$y' = kY \cdot y + kfY \cdot (1 - x - y) + Y_0, \tag{1b}$$

where

$$kX = 1/(1 - \beta - 2\gamma), \tag{2a}$$

$$kY = 1/(1 - \alpha - 2\gamma), \tag{2b}$$

$$kfX = kX \cdot (\gamma - \beta)/(1 - 3\beta), \tag{2c}$$

$$kfY = kY \cdot (\gamma - \alpha)/(1 - 3\alpha), \tag{2d}$$

$$X_0 = -(\beta/(1 - 3\beta) + kX \cdot kfX), \tag{2e}$$

$$Y_0 = -(\alpha/(1 - 3\alpha) + kY \cdot kfY), \tag{2f}$$

where α, β, and γ are the capacitive coupling constants between electrode W-Z, S-Z, and W-S, respectively, and for the wedge and strip anode, $\alpha \approx \beta > \gamma$.

The second correction method is the global correction. When we consider a polynomial degree as three, the function can be written as

$$\begin{bmatrix} x_c \\ y_c \end{bmatrix} = \begin{bmatrix} a_{0x} + a_{1x}x_d + a_{2x}y_d + a_{3x}x_dy_d + a_{4x}x_d^2 + a_{5x}y_d^2 + a_{6x}x_d^2y_d + a_{7x}y_d^2x_d + a_{8x}x_d^3 + a_{9x}y_d^3 \\ a_{0y} + a_{1y}x_d + a_{2y}y_d + a_{3y}x_dy_d + a_{4y}x_d^2 + a_{5y}y_d^2 + a_{6y}x_d^2y_d + a_{7y}y_d^2x_d + a_{8y}x_d^3 + a_{9y}y_d^3 \end{bmatrix}, \tag{3}$$

where (x_d, y_d) and (x_c, y_c) are the feature points coordinates of the original image and the corrected image respectively. In this letter, the center points of each light spot in a counting image are selected as the feature points. Then, the Eq. (3) is rewritten as a matrix form

$$x_c = \vec{A}\vec{p} = \begin{bmatrix} 1 & x_{d1} & y_{d1} & x_{d1}y_{d1} & x_{d1}^2 & y_{d1}^2 & x_{d1}^2y_{d1} & y_{d1}^2x_{d1} & x_{d1}^3 & y_d^3 \\ 1 & x_{d2} & y_{d2} & x_{d2}y_{d2} & x_{d2}^2 & y_{d2}^2 & x_{d2}^2y_{d2} & y_{d2}^2x_{d2} & x_{d2}^3 & y_{d2}^3 \\ \vdots & \vdots & \vdots & \vdots & \vdots & \vdots & \vdots & \vdots & \vdots & \vdots \\ 1 & x_{dM} & y_{dM} & x_{dM}y_{dM} & x_{dM}^2 & y_{dM}^2 & x_{dM}^2y_{dM} & y_{dM}^2x_{dM} & x_{dM}^3 & y_{dM}^3 \end{bmatrix} \begin{bmatrix} p_1 \\ p_2 \\ \vdots \\ p_{10} \end{bmatrix}, \tag{4a}$$

$$y_c = \vec{A}\vec{q} = \begin{bmatrix} 1 & x_{d1} & y_{d1} & x_{d1}y_{d1} & x_{d1}^2 & y_{d1}^2 & x_{d1}^2y_{d1} & y_{d1}^2x_{d1} & x_{d1}^3 & y_d^3 \\ 1 & x_{d2} & y_{d2} & x_{d2}y_{d2} & x_{d2}^2 & y_{d2}^2 & x_{d2}^2y_{d2} & y_{d2}^2x_{d2} & x_{d2}^3 & y_{d2}^3 \\ \vdots & \vdots & \vdots & \vdots & \vdots & \vdots & \vdots & \vdots & \vdots & \vdots \\ 1 & x_{dM} & y_{dM} & x_{dM}y_{dM} & x_{dM}^2 & y_{dM}^2 & x_{dM}^2y_{dM} & y_{dM}^2x_{dM} & x_{dM}^3 & y_{dM}^3 \end{bmatrix} \begin{bmatrix} q_1 \\ q_2 \\ \vdots \\ q_{10} \end{bmatrix}. \quad (4b)$$

The vectors $\vec{p}$ and $\vec{q}$ can be obtained as[12]

$$\vec{p} = (\vec{A}^{\mathrm{T}}\vec{A})^{-1}\vec{A}^{\mathrm{T}}x_s, \quad (5a)$$

$$\vec{q} = (\vec{A}^{\mathrm{T}}\vec{A})^{-1}\vec{A}^{\mathrm{T}}y_s, \quad (5b)$$

where x_s and y_s are the vectors of the desired values of x_c and y_c. After correction of spatial distortion, coordinates of the pixels in the adjusted image are not always integers and gray level must be assigned to the pixels in the corrected image with reconstruction technique of gray level.

At last, the local correction method is used to correct the original image[13,14],

$$\begin{aligned} x_{c,i} &= a_{0x} + a_{1x}x_{d,i} + a_{2x}y_{d,i} + a_{3x}x_{d,i}y_{d,i}, \\ y_{c,i} &= a_{0y} + a_{1y}x_{d,i} + a_{2y}y_{d,i} + a_{3y}x_{d,i}y_{d,i}, \\ & \qquad i = 1, \cdots, 4, \end{aligned} \quad (6)$$

where $(x_{c,i}, y_{c,i})$ are the corrected coordinates of four adjacent points defining a quadrilateral cell, and $(x_{d,i}, y_{d,i})$ are the coordinates of the corresponding original grid points.

Figures 4(a)—(c) show the corrected images using the physical correction method with the capacitive coupling constants $\alpha = \beta = 0.10$, $\gamma = 0.04$, the global correction method, and the local correction method, respectively. One can find that the gray information of each counting light spot is preserved. Distortion at the edge of the image still exists after physical correction (see Fig. 4(a)). The corrected images by the global correction method and the local correction method give better visual effect both in the interior and at the edge (see Figs. 4(b) and (c)), and the original image is corrected effectively.

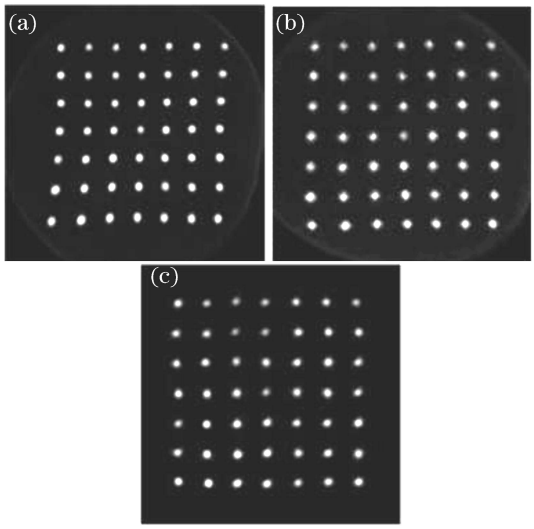

Fig. 4. Corrected images with (a) the physical correction method, (b) the global correction method, and (c) the local correction method.

To evaluate the performance of the three image correction methods furthermore, two parameters, i.e. the position index D and the linearity index L, are defined

$$D = \frac{\sum_{i=1}^{N} \sqrt{(x_i - x_{s,i})^2 + (y_i - y_{s,i})^2}}{N}, \quad (7)$$

$$L = \sum_{i=1}^{m} |(k_r)_i| + \sum_{j=1}^{n} \frac{1}{\left|(k_c)_j\right|}, \quad (8)$$

where (x_i, y_i) and $(x_{s,i}, y_{s,i})$ are the coordinates of the center points of each light spot of the evaluated image and the standard image, respectively. We assume that the image contains $m \times n$ center points and define $N = m \times n$. k_r and k_c are the row slope and the column slope respectively. From the definition, one can see that the position index D describes the position accuracy of a corrected image. A low value of D will indicate that the center points of each light spot in processed image are very adjacent to those of the standard mask, i.e. has little position departure. The linearity index L measures the slope degree of the line formed by the center points of light spots in a same row or column in an image. A low value of L means little linearity departure. One corrected method can be considered to be an effective technique only when its corresponding processing result has both low D and low L.

Figures 5(a)—(e) give the center-point images of the standard image, the original image, and the corrected images respectively. The position index D and the linearity index L are calculated for Figs. 5(b)—(e) and the results are shown in Table 1. From Table 1, one can see that all the correction methods can improve the original image distortion. However, the physical method presents bad position index, which means big position departure. The initial distorted image can not be corrected very validly by the physical correction method. Both the global

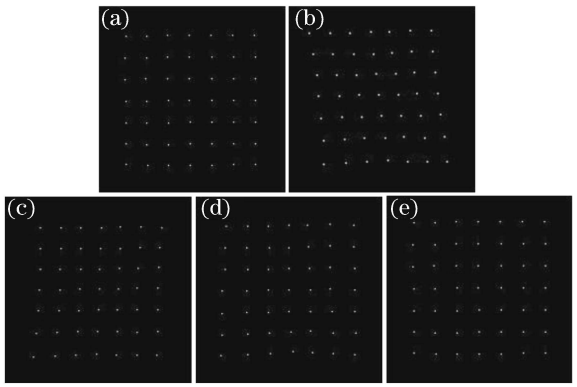

Fig. 5. Center-point images. (a) Standard image; (b) original image; (c) corrected image with the physical correction method; (d) corrected image with the global correction method; (e) corrected image with the local correction method.

Table 1. Performance Evaluation for Each Correction Method

Evaluation Index	Original Image Fig. 3	Physical Correction Fig. 4(a)	Global Correction Fig. 4(b)	Local Correction Fig. 4(c)
D	19.05	16.34	1.40	0.00
L	2.33	0.68	0.43	0.17

correction method and the local correction method can give good values of position index and linearity index, especially the local correction method. There are almost no position departure and little linearity departure in corrected image with the local correction method. In a word, the local correction method can give the most ideal result for the initial distorted image.

In conclusion, the ultraviolet single photon counting imaging system with wedge and strip anode is introduced, the reasons leading to image distortion are analyzed and corresponding measures are implemented to enhance the performance of the single photon imaging system. To improve the quality of the original image further, three correction methods, namely, the physical correction, the global correction, and the local correction, are applied. An ultraviolet single photon counting image obtained by a pinhole mask is tested. The results show that all the correction methods can improve the quality of the initial image without losing gray information of each counting light spot. The local correction method can provide the best visual inspections and performance evaluation values among the three correction methods.

This work was supported by the Knowledge Innovation Program of Chinese Academy of Sciences. X. Zhang's e-mail address is xinghua146@yahoo.com.cn.

References

1. C. Buehler, K. H. Kim, U. Greuter, N. Schlumpf, and P. T. C. So, J. Fluorescence **15,** 41 (2005).
2. H. Li, Optoelectronic Technology (in Chinese) **20,** 45 (2000).
3. S. Wang, Acta Opt. Sin. (in Chinese) **20,** 1072 (2000).
4. B. R. Sandel, A. L. Broadfoot, C. C. Curtis, R. A. King, T. C. Stone, R. H. Hill, J. Chen, O. H. W. Siegmund, R. Raffanti, D. D. Allred, R. S. Turley, and D. L. Gallagher, Space Sci. Rev. **91,** 197 (2000).
5. H. A. MacQueen, C. A. Mattacks, and D. R. Roberts, J. Fluorescence **10,** 301 (2000).
6. R. Civitelli, A. Miyauchi, and K. A. Hruska, J. Tiss. Cult. Meth. **13,** 217 (1991).
7. C. Martin, P. Jelinsky, M. Lampton, R. F. Malina, and H. O. Anger, Rev. Sci. Instrum. **52,** 1067 (1981).
8. D. F. Ogletree, G. S. Balckman, R. Q. Hwang, U. Starke, G. A. Somorjai, and J. E. Katz, Rev. Sci. Instrum. **63,** 104 (1992).
9. J. V. Vallerga, G. C. Kaplan, O. H. W. Siegmund, M. Lampton, and R. F. Malina, IEEE Trans. Nucl. Sci. **36,** 881 (1989).
10. Z. Miao, B. Zhao, Y. Liu, X. Zhu, and X. Zhang, Acta Photon. Sin. (in Chinese) **37,** 11 (2008).
11. Z. Miao, B. Zhao, Y. Liu, and X. Zhu, Acta Photon. Sin. (in Chinese) **36,** 2215 (2007).
12. Y. J. Roh, W. S. Park, and H. Cho, Image and Vision Computing **21,** 1063 (2003).
13. P. Cerveri, C. Forlani, A. Pedotti, and G. Ferrigno, Med. Biol. Eng. Comput. **41,** 151 (2003).
14. D. Soimu, C. Badea, and N. Pallikarakis, Computer. Med. Imag. Graph. **27,** 79 (2003).